Obrabotka metallov (tekhnologiya, oborudovanie, instrumenty) = Metal Working and Material Science. 2024 vol. 26 no. 4 pp. 138–152
ISSN: 1994-6309 (print) / 2541-819X (online)
DOI: 10.17212/1994-6309-2024-26.4-138-152

NSTU NETI

Obrabotka metallov - Metal Working and Material Science

Journal homepage: http://journals.nstu.ru/obrabotka_metallov

Manufacturing of tool electrodes with optimized configuration for copy-piercing electrical discharge machining by rapid prototyping method

Timur Ablyaz [a], ***Vladimir Blokhin*** [b], ***Evgeniy Shlykov*** [c, *], ***Karim Muratov*** [d], ***Ilya Osinnikov*** [e]

Perm National Research Polytechnic University, 29 Komsomolsky prospekt, Perm, 614990, Russian Federation

[a] https://orcid.org/0000-0001-6607-4692, lowrider11-13-11@mail.ru; [b] https://orcid.org/0009-0009-2693-6580, warkk98@mail.ru;
[c] https://orcid.org/0000-0001-8076-0509, Kruspert@mail.ru; [d] https://orcid.org/0000-0001-7612-8025, Karimur_80@mail.ru;
[e] https://orcid.org/0009-0006-4478-3803, ilyuhaosinnikov@bk.ru

ARTICLE INFO

Article history:
Received: 13 September 2024
Revised: 08 October 2024
Accepted: 17 October 2024
Available online: 15 December 2024

Keywords:
Rapid prototyping method
Master model
Precision
Stereolithography
Liquid photopolymer
Copy-and-pierce electrical discharge machining
Flatness deviation

Funding
The research was financially supported by the Russian Science Foundation grant No. 23-79-01224, https://rscf.ru/project/23-79-01224/.

Acknowledgements
The authors express their gratitude to Associate Professor of the department. ITM Federal Autonomous Educational Institution of Higher Education "Perm National Research Polytechnic University" Shumkov A.A. for assistance in obtaining and designing master models by the rapid prototyping method.

ABSTRACT

Introduction. This paper presents the results of obtaining a complex-profile tool electrode (*TE*) for copy-and-pierce electrical discharge machining by casting technology. This method consists in using a master model by rapid prototyping method. ***The purpose of the work*:** experimental study of accuracy assurance in manufacturing of complex-profile *TE* by casting with the use of rapid prototyping technology for copy-piercing electrical discharge machining. **Research Methods.** The master model of *TE* was produced on the *Envisiontec Perfactory XEDE* machine using stereolithography technology. *Si500* photopolymer was used as a starting material. Intermediate and final surface deviation measurements were performed on a *Contura Carl Zeiss G2 CMM*. Calculation of the gutter and feed system was performed in *ProCast* software. A casting was obtained from casting brass *LC40S (Cu-40 Zn-Pb)*. The study of the process of copy-piercing electrical discharge machining of *TE* made by casting with the use of rapid prototyping technology was carried out with the help of *Smart CNC* copy-piercing machine in the environment of transformer oil. Operating parameters: pulse turn-on time (T_{on}, μs), voltage (***U***, V), current (***I***, A). **Results and discussion.** The methodology of design and manufacturing of complex-profile *TE* with application of rapid prototyping technology for copy-piercing electrical discharge machining is developed. The analysis of shape deviation shows that errors occur during the manufacturing of the master model by stereolithography. An experimental study of the shape deviation of the master model shows surface concavity in the range of 0.03 to 0.07 mm depending on the arrangement of the sides. It is shown that the optimized master model has 25 % less shape deviation. A sprue-feeding system (*SFS*) is developed for the fabrication of *TE* by casting technology. When porosity is evaluated, it is found that pores are concentrated in the *SFS* and riser, which positively affects the quality of the casting. Manufacturing of the tool electrode with the help of casting technology showed that all accuracy and roughness parameters are within the specified tolerance and correspond to the initial drawing data. Experimental study of the process of electroerosion machining of the profile groove of the *TE* manufactured by casting on the investment casting model obtained with the use of rapid prototyping technology is carried out. It is established that the dimensions of the obtained groove meet the stated requirements.

For citation: Ablyaz T.R., Blokhin V.B., Shlykov E.S., Muratov K.R., Osinnikov I.V. Manufacturing of tool electrodes with optimized configuration for copy-piercing electrical discharge machining by rapid prototyping method. *Obrabotka metallov (tekhnologiya, oborudovanie, instrumenty) = Metal Working and Material Science*, 2024, vol. 26, no. 4, pp. 138–152. DOI: 10.17212/1994-6309-2024-26.4-138-152. (In Russian).

*** Corresponding author**
Shlykov Evgeniy S., Ph.D. (Engineering), Associate Professor
Perm National Research Polytechnic University,
29 Komsomolsky prospect,
614990, Perm, Russian Federation
Tel.: +7 961 759-88-49, **e-mail**: Kruspert@mail.ru

Introduction

Machining is used to produce complex profile surfaces. This method has a number of technological and economic disadvantages. To obtain different profiles, it is necessary to manufacture different profile cutting tools that are applicable in one technological transition. Under such conditions, the production cycle of the product increases due to frequent tool changes. When providing the required surface profile, it is mainly required to use equipment with the possibility of multi-axis machining, which leads to an increase in the cost of the product [1–3].

Copy-piercing electrical discharge machining (*CPEDM*) is widely used to produce complex profile surfaces. *CPEDM* allows obtaining the profile of products of various shapes with minimal expenditures on tools and tooling. Technological transitions do not require the use of special tooling due to the absence of cutting forces in the process of *CPEDM* [4–7].

The efficiency of *CPEDM* depends on the quality of the tool electrode (*TE*). In modern production, complex profile *EDMs* are produced by machining methods (turning, milling). The required surface contour often makes demand for *TE* that cannot be produced by three-axis machining and then *TE* is produced on five-axis machining centers with the use of special tooling and cutting tools. These methods of *TE* manufacturing require significant economic and time expenditures. It is not reasonable to use it within the framework of mass production. For pilot production it is characteristic to produce one test sample for making subsequent changes in its design to minimize the production cycle to ensure the required result.

A relevant solution is the production of complex-profile *TE* using investment casting technology with obtaining a master model using the rapid prototyping method. The rapid prototyping technology allows producing a prototype of *TE* to assess the quality and quickly correct the product model. The use of additive technologies to obtain a master model makes it possible to manufacture single *TE* of different profiles in a short time. Modern equipment used in additive manufacturing allows producing a batch of *TE* with different profiles in one production cycle, which helps to reduce economic costs and shorten the production cycle [8].

Literature analysis [9–11] showed that it is possible to produce prototypes of products with minimal deviations and structural defects using the technology of rapid prototyping from liquid photopolymers. The application of this technology allows providing the required parameters of repeatable geometry of complex-profile elements. The works [12–16] note the effectiveness of this technology for obtaining the required complex-profile products. However, the issue of the accuracy of master models obtained by stereolithography has not been fully studied at present.

The actual task is the development of scientifically substantiated approaches for manufacturing of complex-profile ET by alternative technologies.

The purpose of the work is to ensure the accuracy of manufacturing of complex-profile *TE* by casting with the use of rapid prototyping technology for copy-piercing electrical discharge machining.

Objectives:

1) to develop a methodology for designing and manufacturing complex-profile *TE* for *CPEDM* using rapid prototyping technology to create a master model;

2) to analyze the shape deviations of a master model made of liquid photopolymer using a coordinate measuring machine (*CMM*);

3) to perform *CAD* model correction to reduce the shape deviation of the master model;

4) to develop a sprue-feeding system and evaluate the porosity of the casting during metal pouring;

5) to conduct an experimental study of the accuracy of the *CPEDM* process of the profile groove of the *TE* made by casting with obtaining the investment pattern using the rapid prototyping technology.

Research methodology

The experiments were conducted on the basis of the Center for Collective Usage of the Department of "Innovative technologies of mechanical engineering" of the Federal Autonomous Educational Institution of Higher Education "Perm National Research Polytechnic University". Within the framework of the research

5 samples of tool-electrodes for *CPEDM* of a blind profile groove in special-purpose products were produced using investment casting method; a sketch of the *TE* is presented in Fig. 1. *The* tool-electrodes were designed taking into account the inter-electrode gap (*IEG*) calculated according to the methodology presented in [17, 18].

CAD-model with sprue-feeding system was designed in *SOLIDWORKS* computer-aided design system.

Processing of the *CAD*-model for the production of investment pattern by stereolithography (*SLA*) method was carried out using the *Materialles Magics* software package. The design of supports (Fig. 2) is necessary for free removal from the working place of construction. To minimize cost of *SLA* production, the internal filling of the *TE* was performed with a cellular structure of a *Wigner – Seitz* face-centered cubic lattice (Fig. 2). This type of lattice holds equiaxial loading well, which allows obtaining a master model with acceptable shape deviations after post-polymerization of the material in air [19–21].

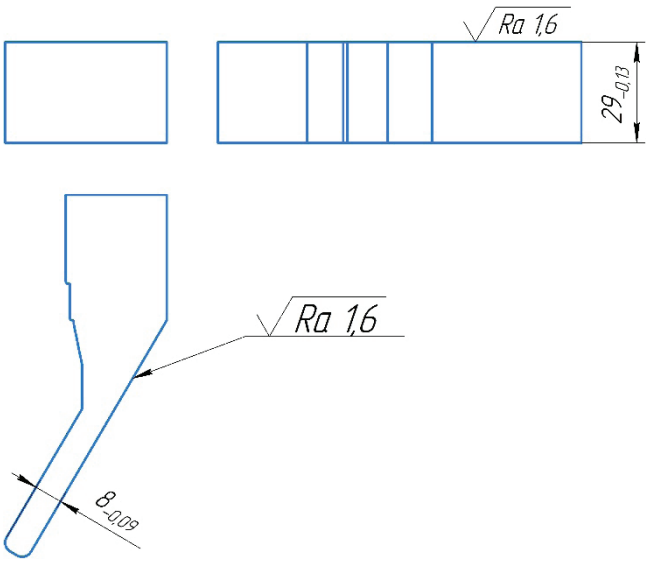

Fig. 1. Sketch of the tool electrode

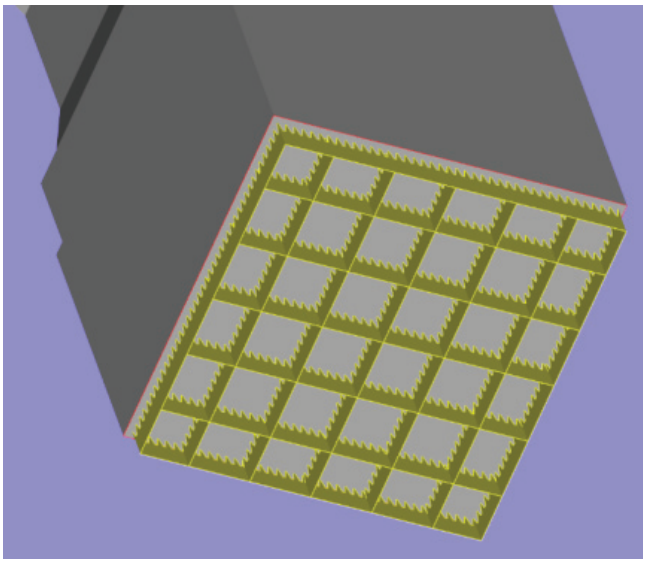

Fig. 2. Supports for *TE*

Growing of *TE* was carried out on a mask-type *Envisiontec Perfactory XEDE* unit. The mode parameters are presented in Table 1.

The patterns were manufactured using a photopolymer material based on acrylates (*Si500*), which belongs to the class of cross-linked polymers. The characteristics of the material under normal conditions are presented in Table 2.

The *CAD* model of the *TE* prototype with a sprue-feeding system (*SFS*) is shown in Fig. 3.

The *ProCast* software package was used to calculate the *SFS*.

When designing the *SFS*, it is necessary to take into account the following:

1) identical conditions for each section of the casting during casting;

2) for thick-walled sections, the presence of an additional depot of liquid metal in order to eliminate defects (shrinkage cavities, weakness and porosity in the metal);

Table 1

Parameters of the build mode of the investment pattern by *SLA* method

Parameter	Value
Layer thickness, μm	50
Supports height, mm	3
Thickness of supports, μm	280
Time of illumination of model section and supports, ms	8,500

Table 2

Characteristics of *Si500* photopolymer material under normal conditions

Parameter	Value
Tensile modulus of elasticity (*E*), MPa	2.68
Ultimate strength (σ), MPa	78.1
Relative strain (ε), %	4.39
Bending strength (σ), MPa	65
Glass transition temperature (*T*), °C	61
Density in liquid state (ρ), g/cm^3	1.1
Density in solid state (ρ), g/cm^3	1.2

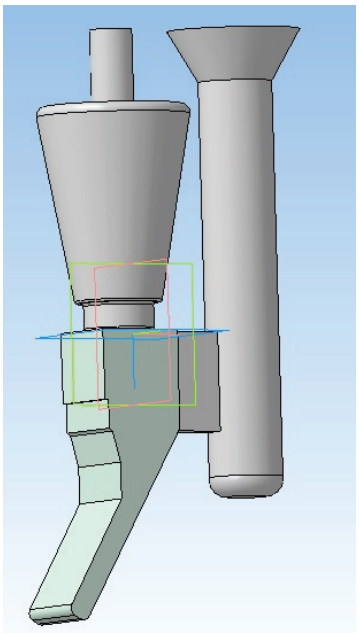

Fig. 3. TE model with sprue-feeding system

3) the direction of hot metal from thick-walled sections to thin-walled ones.

After the master model was made for each *TE*, a model kit of *SFS* and a casting model from casting wax were formed using a silicone mold.

The obtained wax models of the electrodes were connected with *SFS*. The wax *TE*s with *SFS* were then mounted in a mold and filled with gypsum. The mold was calcined to a temperature of 750 °C. After the mold cooled down to a temperature of 450 °C, the models were calcined in an induction crucible furnace, and then the castings were removed from the mold. The material used was foundry brass *Cu*-40 *Zn-Pb*.

Master models as well as wax models and subsequent castings were measured on a *Contura Carl Zeiss G2* three-axis *CMM*. Shape deviations and the magnitude of possible corrections were considered.

The samples under study were mounted perpendicular to the plane of the table, and the displacements relative to the cross-section of the vertical and horizontal surfaces of the prototype were measured. Four surfaces were measured on each obtained *TE*. The measured surfaces and the measurement strategy are shown in Fig. 4.

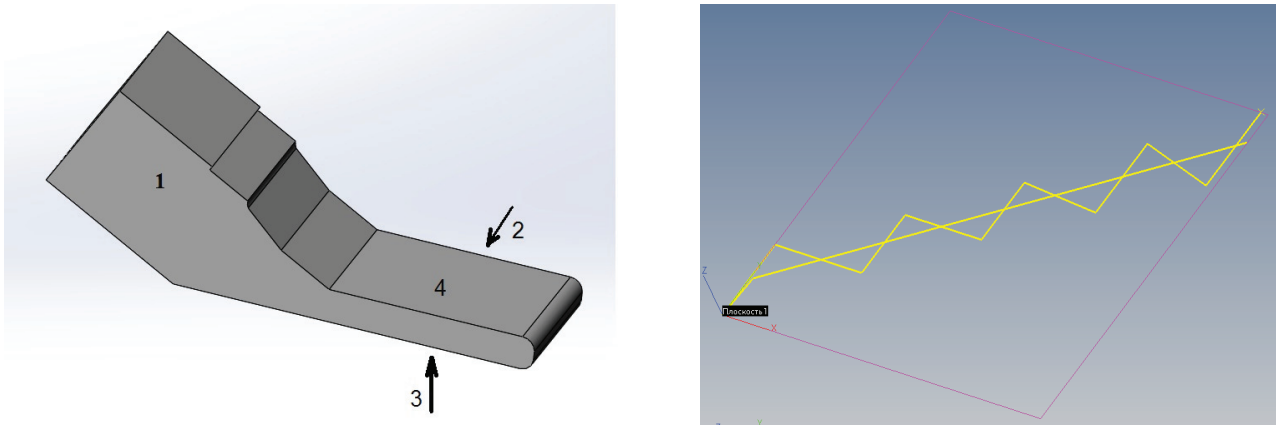

a *b*

Fig. 4. Measured surfaces of the tool electrodes (*a*) and the trajectory of measuring the *TE* (*b*)

The measurement strategy is a polyline. The measurement was performed in such a way as to maximize the use of the entire surface. As a result, statistics from 200 points in three ***x***, ***y***, ***z*** coordinates were collected.

To test the obtained metallic *TE*, an experiment was conducted on *CPEDM* of steel 45 (0.45 % *C*). The processing was performed on a *CPEDM Smart CNC* machine in the environment of industrial oil grade *I-20a GOST 982-80*.

The *CPEDM* mode is presented in Table 3.

Table 3

Machining mode on the copy-piercing *EDM* machine

Parameters	Values
	max
I, A	8
U, V	50
T_{on}, μs	100

Results and discussion

Fig. 5 shows the cellular structure of the internal filling of the investment patterns.

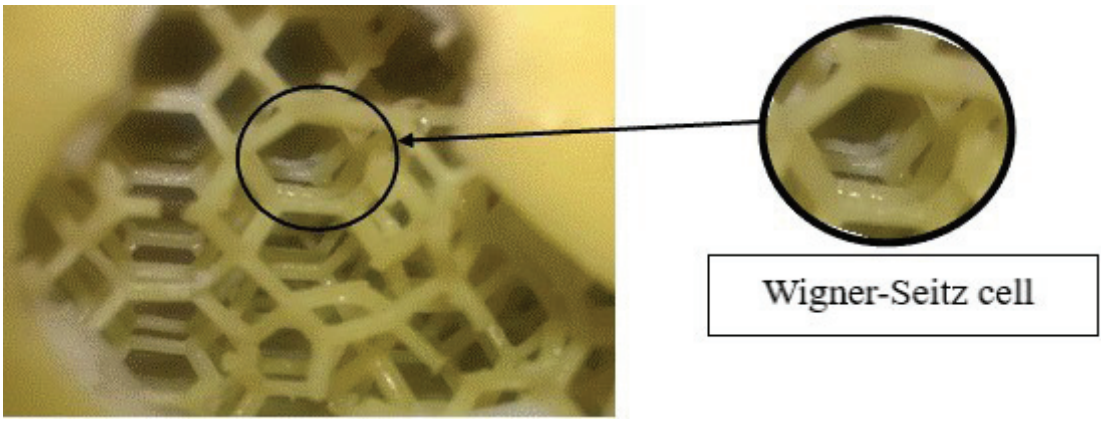

Fig. 5. Cell filling with the structure of a face-centered *Wigner-Seitz* cubic lattice

The *Calypso* software package shows the average flatness deviations on surfaces 1–4 (Fig. 6) of all five *TE* samples. The approximation method was used to model the flatness deviation error line.

A data sampling of twelve points for each plane was made for visualization. The points were selected on the measurement line where it breaks.

The sampling data for surface **1** is presented in Table 4.

The location of these points is shown in Fig. 7. An approximation line is drawn through these points, indicating the average actual size of the master models.

Table 5 shows the flatness deviations of the samples of all measured surfaces and the average value. It is necessary to take these deviations into account and add it to the original *CAD* model to create a new geometry of the part.

To eliminate the resulting deviation, a new dimension is calculated that compensates for the shape deviation and is equal to the average size of the flatness deviation. Fig. 8 shows the changes in the part shape geometry on surfaces **1**–**4**.

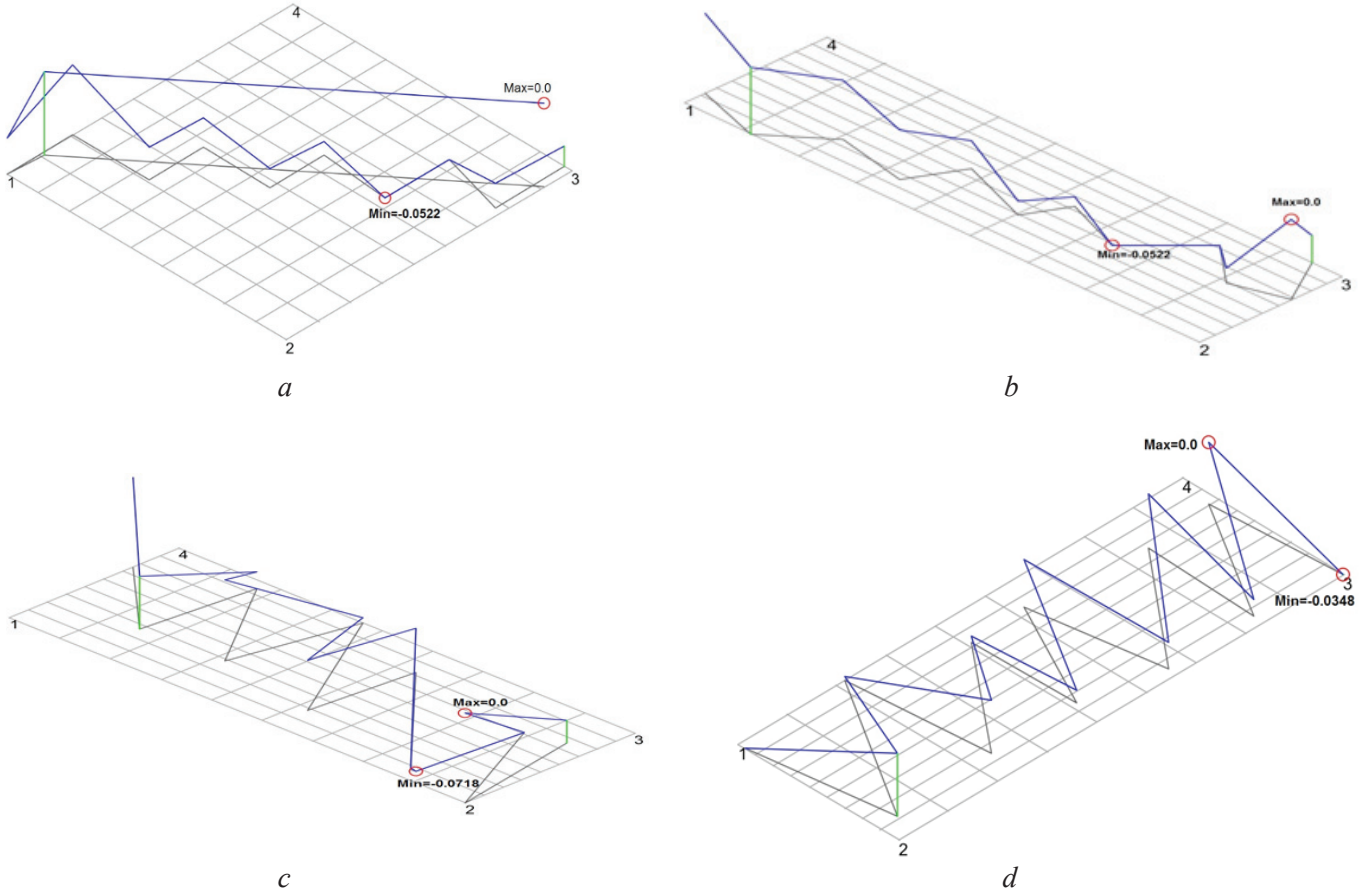

a *b* *c* *d*

Fig. 6. Measurement trajectory with the value of average flatness deviation along the surface:
a – 1; *b* – 2; *c* – 3; *d* – 4

Table 4

Sampling points from surface 1

Surface	Point	Coordinates of points on the surface 1		
		X	***Y***	***Z***
1	1	264.2598	−513.1588	−477.3192
	2	264.2567	−518.4794	−477.3239
	3	259.5628	−517.3288	−477.2899
	4	259.5518	−521.9996	−477.2986
	5	255.7281	−520.0690	−477.2837
	6	255.7163	−525.1954	−477.2634
	7	250.7091	−523.9416	−477.2420
	8	250.6929	−529.7544	−477.2196
	9	244.3490	−528.7445	−477.1874
	10	244.3337	−534.6175	−477.1713
	11	237.7511	−536.6551	−477.1053
	12	267.6178	−513.1320	−477.3031

The End Table 4

Surface	Point	Coordinates of points on the surface 1		
		X	***Y***	***Z***
2	1	266.8592	−536.3874	−477.330
	2	266.8582	−539.1545	−477.2888
	3	262.9658	−539.3621	−477.3156
	4	258.9135	−542.0315	−477.2840
	5	254.9696	−539.4720	−477.2727
	6	250.3227	−541.9105	−477.2169
	7	245.5120	−543.7889	−477.1600
	8	237.8660	−544.3309	−477.1061
	9	230.9308	−544.0254	−477.0633
	10	227.6826	−544.4671	−477.0632
	11	234.7477	−544.6761	−477.0746
	12	236.7347	−543.6066	−477.0987
3	1	268.8741	−517.3798	−479.1381
	2	268.7148	−517.5176	−488.4096
	3	266.4900	−519.2954	−481.6966
	4	266.5182	−519.2315	−489.1544
	5	262.5285	−522.4333	−481.4241
	6	262.0909	−522.7745	−489.2207
	7	259.3579	−524.9424	−484.7519
	8	258.9885	−525.2224	−489.5129
	9	252.9817	−529.9868	−481.4362
	10	254.9560	−528.4201	−48.5392
	11	249.1152	−533.0230	−482.6272
	12	242.8281	−538.0595	−489.9179
4	1	264.0658	−510.4802	−481.0604
	2	263.1891	−511.1592	−490.5512
	3	260.0128	−513.6948	−481.1179
	4	258.2810	−515.0385	−488.8638
	5	253.7875	−518.5229	−482.0872
	6	253.1226	−519.1440	−490.6190
	7	249.1201	−522.2798	−481.9732
	8	249.2972	−522.1993	−491.0848
	9	245.1400	−525.4132	−481.5228
	10	242.5907	−527.4970	−491.0312
	11	237.5517	−531.5133	−490.5426
	12	236.7127	−532.0627	−481.5488

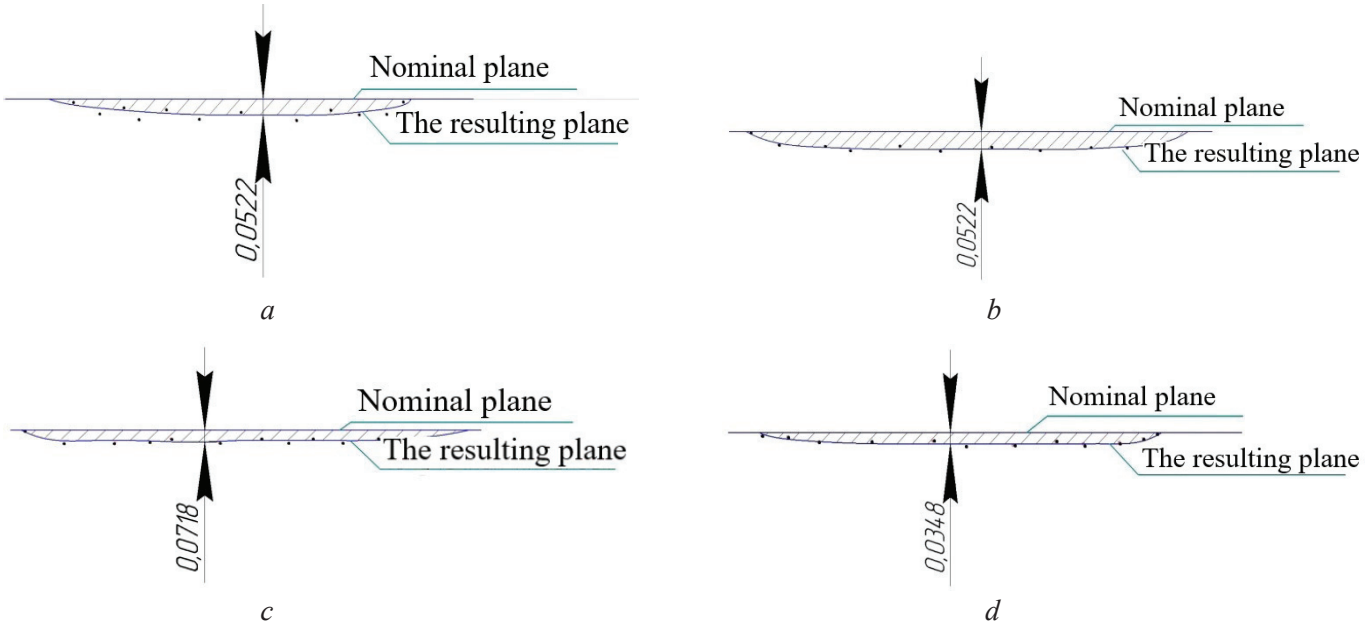

Fig. 7. Average flatness deviation on the surface:
a – 1; *b* – 2; *c* – 3; *d* – 4

Table 5

Flatness deviation (mm)

Sample No.	Surfaces			
	1	2	3	4
1	0.0517	0.0512	0.0715	0.0346
2	0.0528	0.0519	0.0717	0.0341
3	0.0523	0.0519	0.0720	0.0352
4	0.0521	0.0529	0.0710	0.0351
5	0.0521	0.0530	0.0724	0.0351
Average value	0.0522	0.0522	0.0718	0.0348

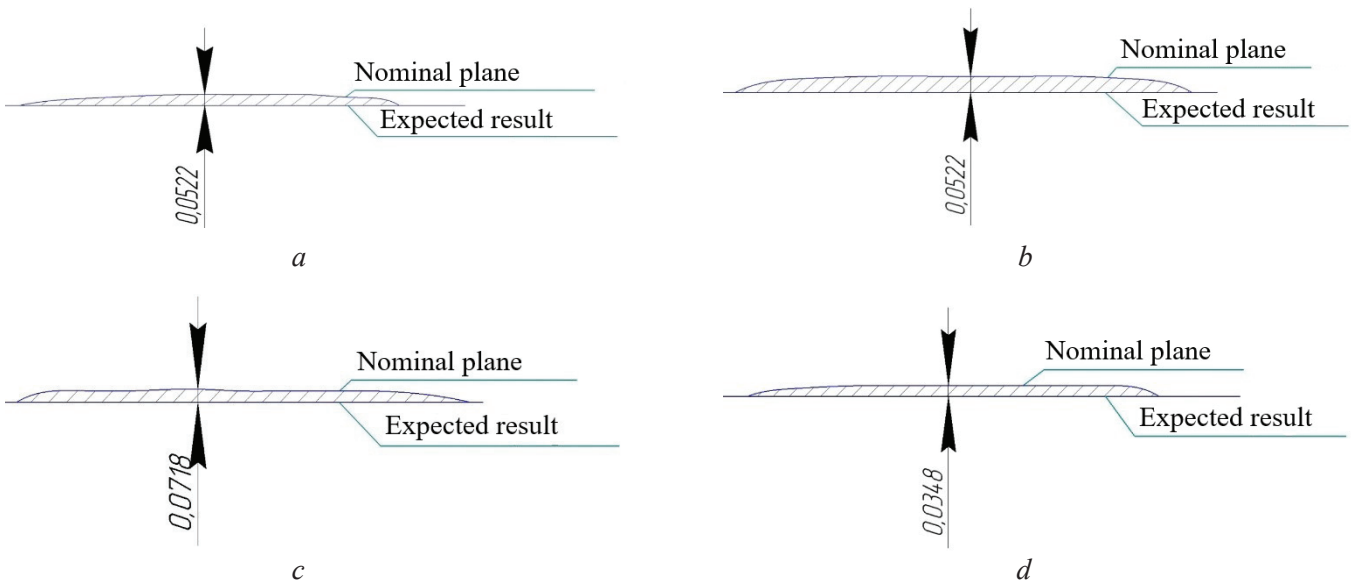

Fig. 8. Assumed geometry of the shape on the surface:
a – 1; *b* – 2; *c* – 3; *d* – 4

The calculated nominal dimensions are added into the *CAD* model (Fig. 9), and a new geometry of surfaces **1**–**4** is created.

After the changes were made, the master models were re-grown on the original mode. Master models were grown vertically. Supports were located on the non-working part of the electrode. Repeated measurements of flatness deviations of all surfaces of the master models were performed. Table 6 shows the repeated measurements of the *TE* models.

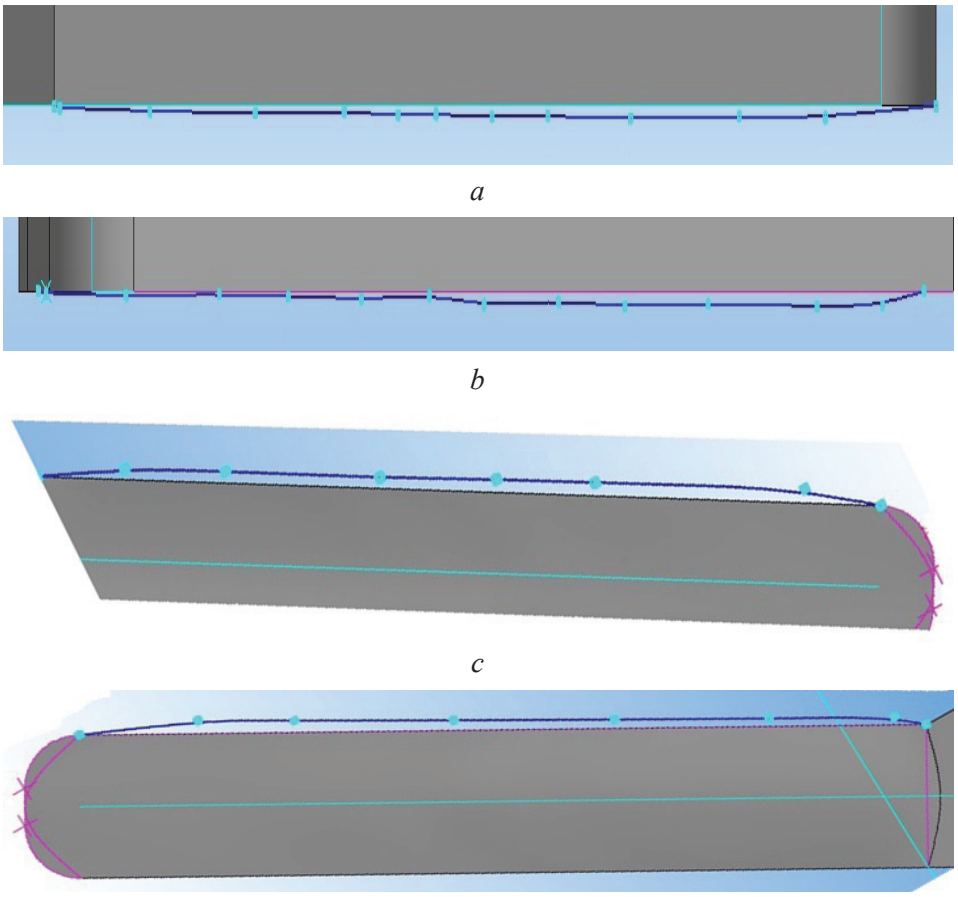

a

b

c

d

Fig. 9. Modified geometry of the mold taking into account the performed calculations on the surface:

a – 1; *b* – 2; *c* – 3; *d* – 4

Table 6

Measurements of *TE* models after re-build

TE No.	**Surfaces**			
	1	**2**	**3**	**4**
1	0.0388	0.0400	0.0539	0.0301
2	0.0394	0.0382	0.0549	0.0305
3	0.0394	0.0395	0.0538	0.0309
4	0.0397	0.0399	0.0530	0.0311
5	0.0387	0.0385	0.0538	0.0314
Average value	0.0392	0.0392	0.0539	0.0308

The analysis of the obtained data shows a decrease in the average deviation of master model growth by 25 % of the first, second and third surfaces. The flatness deviation of surface **4** decreased by 11.5 % due to the smaller surface area and the smaller angle of its location relative to the table.

When making a casting, the mold was filled with melt through a slot feeder. As the melt entered the thin areas of the casting, the cooling rate was equalized and gas was removed from the casting. This ensures that there are no shrinkage pores in the body of the *TE* casting.

The distribution of pores in feed and sprue system calculated in the *ProCast* software is shown in Fig. 10. The entire model has about 13 % porosity. It is found that the defect does not affect the critical part of the casting of the part. This fact improves the surface quality and density of the metal. The program performs calculations under ideal conditions. Actual results may differ from the calculations.

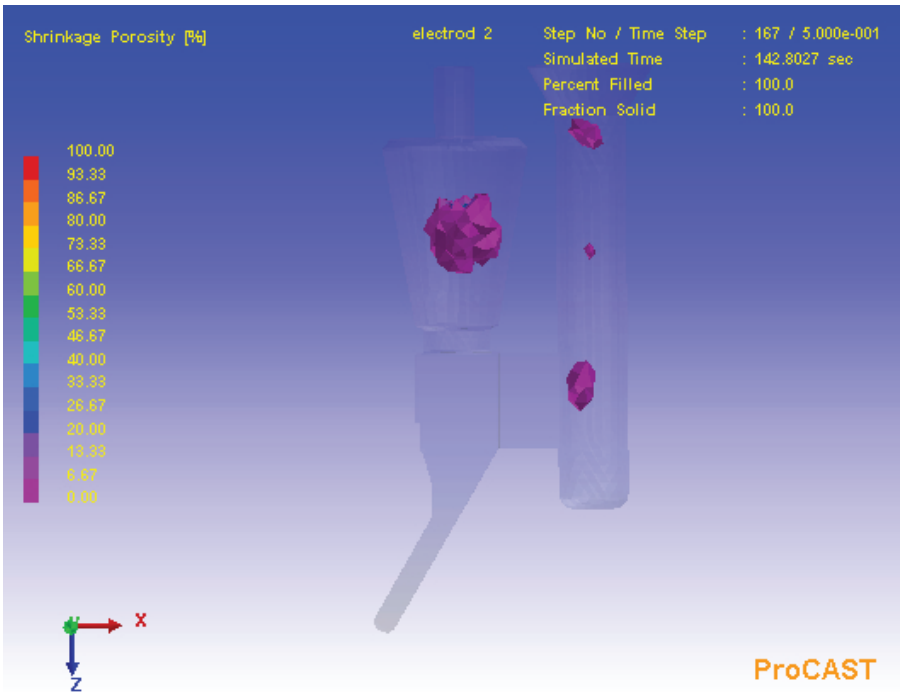

Fig. 10. Porosity distribution in the body of the part casting

Based on the calculation performed, the correctness of the designed casting and *SFS* is proved.

Fig. 11, *a* shows the master model after correction; the wax model is shown in Fig. 11, *b*. Fig. 11, *c* shows the metal casting with *SFS*, which is separated from the part by a cutoff tool. Metal *TE* with the fixing method and the corresponding groove profile machined by copy-piercing electrical discharge machining method with the obtained metal *TE* are presented in Figs. 11, *g–f*.

During the experiment, a master model, a wax model, and a metal casting were obtained. Table 7 shows the specified dimensions and roughness of the *CAD* model and the data obtained by measuring the metal casting.

The obtained dimensions and roughness of the metal casting satisfy the specified parameters.

According to the results of the experimental study of the use of *TE,* manufactured using the casting technology with the use of rapid prototyping method to obtain a master model, the surface quality of the profile groove meets the requirements of the drawing. The taken into account interelectrode gap (*IEG*) allows for dimensions within the 12th accuracy degree, which meets the requirements of pilot production.

Conclusions

1. A methodology for designing and manufacturing a complex-shaped *TE* using rapid prototyping technology for copy-piercing electrical discharge machining is developed.

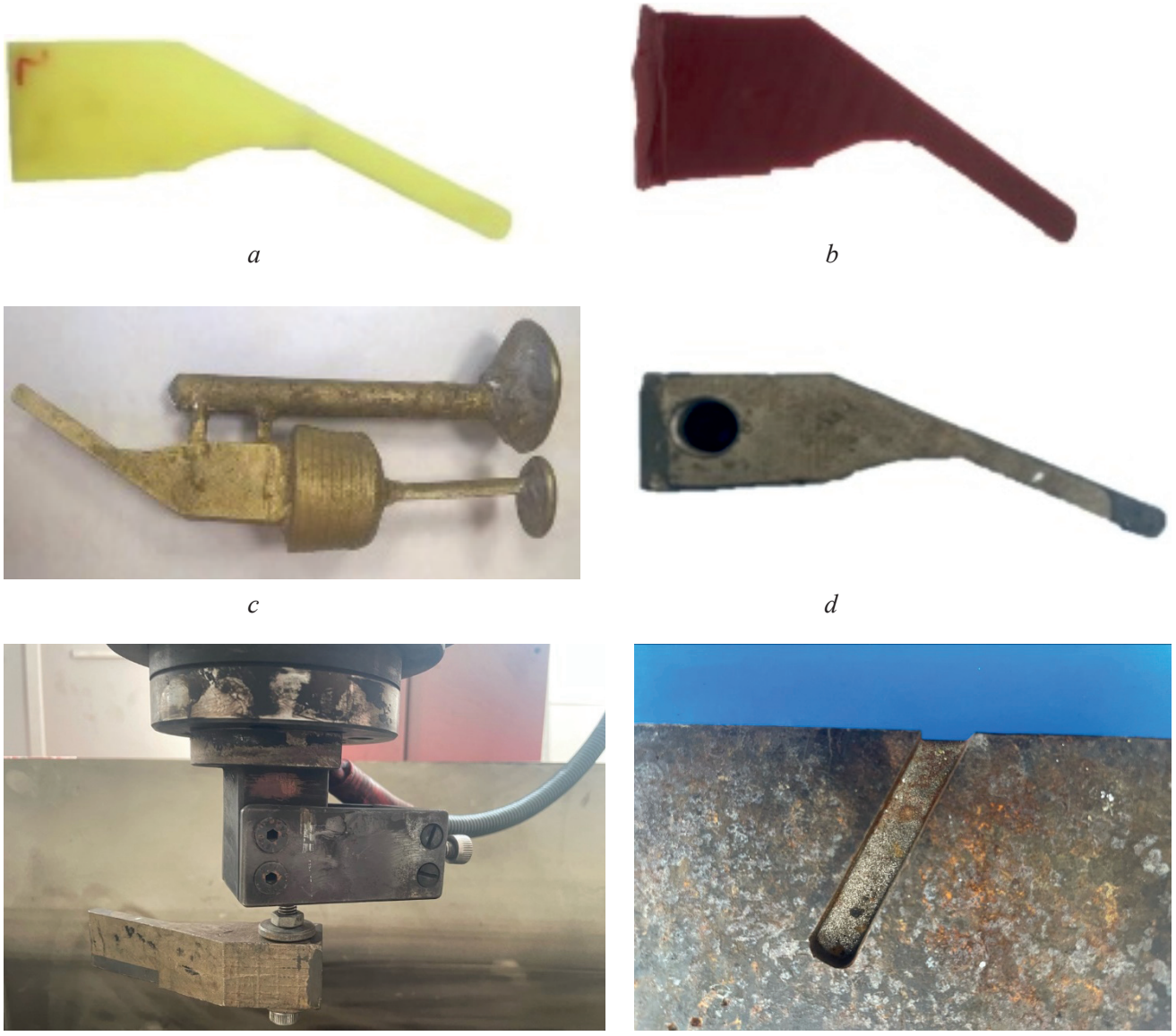

a *b*

c *d*

e *f*

Fig. 11. Technological process of *TE* manufacturing:

a – master model; *b* – wax model; *c* – metal casting with *SFS*; *d* – *TE*; *e* – *TE* with fixing; *f* – mating profile of groove surface after *CPEDM*

Table 7

Comparative table of measurement results

	Dimensions (mm)		Roughness (μm)	
	Sides 1–2	Sides 3–4	Sides 1–2	Sides 3–4
CAD model	$29_{-0.13}$	$8_{-0.09}$	Ra 1.6	Ra 1.6
Metal casting	28.90	7.98	Ra 1.6	Ra 1.6

2. Analysis of shape deviations has shown that errors occur when manufacturing a master model using stereolithography.

3. An experimental study of the shape deviation of the master model has shown a surface concavity in the range from 0.03 to 0.07 mm depending on the location of the sides.

4. It is shown that the optimized master model has 25 % fewer shape deviations.

5. A feed and sprue system is developed for manufacturing *TE* using casting technology. When evaluating the porosity, it is found that the pores are concentrated in the feed and sprue system, which has a positive effect on the quality of the casting.

6. Manufacturing a tool-electrode using casting technology has shown that all the accuracy and roughness parameters of the *TE* are within the specified tolerance and correspond to the original data of the drawing.

7. An experimental study is conducted of the process of electrical discharge machining of a profile groove with a tool-electrode, which was manufactured by the method of investment casting using an investment pattern obtained using rapid prototyping technology. It is found that the dimensions of the resulting groove meet the stated requirements.

References

1. Su X., Wang G., Yu J., Jiang F., Li J., Rong Y. Predictive model of milling force for complex profile milling. *The International Journal of Advanced Manufacturing Technology*, 2016, vol. 87, pp. 1653–1662. DOI: 10.1007/s00170-016-8589-1.

2. Sommer D., Safi A., Esen C., Hellmann R. Additive manufacturing of Nickel-based superalloy: optimization of surface roughness using integrated high-speed milling. *Proceedings of SPIE*, 2024, vol. 12876. *Laser 3D Manufacturing XI*. DOI: 10.1117/12.3000972.

3. Gimadeev M.R., Nikitenko A.V., Berkun V.O. Influence of the sphero-cylindrical tool orientation angles on roughness under processing complex-profile surfaces. *Advanced Engineering Research*, 2023, vol. 23 (3), pp. 231–240. DOI: 10.23947/2687-1653-2023-23-3-231-240.

4. Ho K.H., Newman S.T. State of the art electrical discharge machining (EDM). *International Journal of Machine Tools and Manufacture*, 2003, vol. 43 (13), pp. 1287–1300. DOI: 10.1016/S0890-6955(03)00162-7.

5. Porwal R.K., Yadava V., Ramkumar J. Micro electrical discharge machining of micro-hole. *Advanced Science Engineering and Medicine*, 2020, vol. 12 (11), pp. 1335–1339. DOI: 10.1166/asem.2020.2586.

6. Rajurkar K.P., Sundaram M.M., Malshe A.P. Review of electrochemical and electrodischarge machining. *Procedia CIRP*, 2013, vol. 6 (2), pp. 13–26. DOI: 10.1016/j.procir.2013.03.002.

7. Rathod R., Kamble D., Ambhore N. Performance evaluation of electric discharge machining of titanium alloy – a review. *Journal of Engineering and Applied Science*, 2022, vol. 69 (1), pp. 1–19. DOI: 10.1186/s44147-022-00118-z.

8. Melchels F.P.W., Feijen J., Grijpma D.W. A review on stereolithography and its applications in biomedical engineering. *Biomaterials*, 2010, vol. 31, pp. 6121–6130. DOI: 10.1016/j.biomaterials.2010.04.050.

9. Tumbleston J.R., Shirvanyants D., Ermoshkin N., Janusziewicz R., Johnson A.R., Kelly D., Chen K., Pinschmidt R., Rolland J.P., Ermoshkin A., Samulski E.T., DeSimone J.M. Continuous liquid interface production of 3D objects. *Science*, 2015, vol. 6228 (347), pp. 1349–1352. DOI: 10.1126/science.aaa2397.

10. Shusteff M., Browar A.E.M., Kelly B.E., Henriksson J., Weisgraber T.H., Panas R.M., Fang N.X., Spadaccini C.M. One-step volumetric additive manufacturing of complex polymer structures. *Science Advances*, 2017, vol. 3 (12), pp. 1–7. DOI: 10.1126/sciadv.aao5496.

11. Janusziewicza R., Tumblestonb J.R., Quintanillac A.L., Mechama S.J., DeSimonea J.M. Layerless fabrication with continuous liquidinterface production. *Proceedings of the National Academy of Sciences,* 2016, vol. 113 (42), pp. 1–6. DOI: 10.1073/pnas.1605271113.

12. Han D., Yang C., Fangb N.X., Lee H. Rapid multi-material 3D printing with projection micro-stereolithography using dynamic fluidic control. *Additive Manufacturing*, 2019, vol. 27 (17), pp. 606–615. DOI: 10.1016/j.addma.2019.03.031.

13. Jigang H., Qin Q., Jie W. A review of stereolithography: processes and systems. *Processes*, 2020, vol. 8 (9), pp. 1–16. DOI: 10.3390/pr8091138.

14. Ligon S.C., Liska R., Stampfl J., Gurr M., Mülhaupt R. Polymers for 3D printing and customized additive manufacturing. *Chemical Reviews,* 2017, vol. 117 (15). DOI: 10.1021/acs.chemrev.7b00074.

15. Stansbury J.W., Idacavage M.J. 3D printing with polymers: challenges among expanding options and opportunities. *Dental Materials*, 2016, vol. 32 (1), pp. 54–64. DOI: 10.1016/j.dental.2015.09.018.

16. Wang X., Jiang M., Zhou Z., Gou J., Hui D. 3D printing of polymer matrix composites: a review and prospective. *Composites, Part B: Engineering*, 2017, vol. 110, pp. 442–458. DOI: 10.1016/j.compositesb.2016.11.034.

17. Golabczak A., Konstantynowicz A., Golabczak M. Mathematical modelling of the physical phenomena in the interelectrode gap of the EDM process by means of cellular automata and field distribution equations. *Experimental and Numerical Investigation of Advanced Materials and Structures*. Cham, Springer, 2013, pp. 169–184. DOI: 10.1007/978-3-319-00506-5_11.

18. Kumar A., Mandal A., Dixit A.R., Mandal D.K. Quantitative analysis of bubble size and electrodes gap at different dielectric conditions in powder mixed EDM process. *The International Journal of Advanced Manufacturing Technology*, 2020, vol. 4 (1), pp. 1–11. DOI: 10.1007/s00170-020-05189-x.

19. Kilina P.N., Vasilyuk V.P., Morozov E.A., Khanov A.M., Sirotenko L.D. Using rapid prototyping technologies for creating implants with cellular structure. *Biosciences Biotechnology Research Asia*, 2015, vol. 12 (2), pp. 1691–1698. DOI: 10.13005/bbra/1832.

20. Yin F., Koskinen P., Kulju S., Akola J., Palmer R.E. Real-space wigner-seitz cells imaging of potassium on graphite via elastic atomic manipulation. *Scientific Reports*, 2015, vol. 5 (1), pp. 1–5. DOI: 10.1038/srep08276.

21. Cho Y., Lee I., Cho D.W. Laser scanning path generation considering photopolymer solidification in micro-stereolithography. *Microsystem Technologies*, 2005, vol. 11 (2), pp. 158–167. DOI: 10.1007/s00542-004-0468-2.

Conflicts of Interest

The authors declare no conflict of interest.